

A METHODOLOGY FOR ESTIMATING THE RADIATION PATTERN OF A VIOLIN DURING THE PERFORMANCE

Antonio Canclini, Luca Mucci, Fabio Antonacci, Augusto Sarti, and Stefano Tubaro

Politecnico di Milano, Dipartimento di Elettronica, Informazione e Bioingegneria, Milano, Italy

ABSTRACT

We propose a method for the estimation of the three-dimensional radiation pattern of violins, during the performance of a musician. A microphone array captures the energy radiated by the violin in different directions using beamforming based on sub-arrays. The 3D radiation pattern is estimated allowing the musician to freely move. In particular, a tracking system estimates the position and orientation of the violin. The adopted system can be also used in a mildly reverberant environment, thus allowing the musician to play in a natural fashion. The experimental results prove the accuracy and the effectiveness of the method.

Index Terms— Musical acoustics, plenacoustic analysis, radiation pattern

1. INTRODUCTION

Several acoustic properties of the violin are studied. A particularly interesting one is the *directivity* or *radiation pattern*, which gives the angular dependency of the sound energy radiated from the instrument in the far field. The knowledge of the directivity allows us to infer how the sound will interact with the environment. The radiation pattern of the violin is a complex function that depends on several factors (e.g., materials and shapes), and it is difficult to predict, as shown in [1], and subtleties related to it can arise complex phenomena such as the “directional tone color” [2], which cause different notes to be perceived as coming from different directions.

In this paper we propose a methodology for measuring the radiation pattern during the performance. Several techniques have been proposed in the literature. Most of them are based on artificial excitation mechanisms: in [2] loudspeakers are adopted for exciting the violin; a force hammer is used in [3]; while the method in [4] relies on a mechanical bowing machine. Despite being characterized by a controlled and repeatable excitation of the instrument, these methods do not consider the effect of human body on sound radiation. In order to account for the modifications introduced by the human body,

other systems measure the directivity pattern of an instrument played by a violinist. In [5] a large semicircular microphone array is used to measure the sound radiated by a violin, while the player sits on a rotating stool. In [6] the musician stands at the center of an anechoic room, holding the violin in a prescribed position, and the acoustic energy is measured at 22 points surrounding it. A similar approach is followed in [7], where a scanning probe microphone is used to measure the soundfield over planar regions. In [8] the violin is also kept still on a rigid structure. Unfortunately, this solution prevents the musician to play in a natural fashion.

All the mentioned techniques rely on measurements conducted in anechoic rooms, which ensure to capture the sole direct sound radiation. This scenario, while ideal in case of artificial excitation, presents some issues for the violinist. Indeed, it exposes the player only to the dry violin sound, which typically provokes an annoying sensation that may impact on the naturalness of the performance. In this paper we propose a novel technique for measuring the 3D radiation pattern of a violin. A compact rectangular microphone array (plenacoustic camera) is used to sense the directional components of the wave field. This is accomplished by the plenacoustic analysis of the wavefield proposed in [9], useful to estimate the directional acoustic energy at multiple points in space. This analysis is based on beamforming, and enables the measurement of the radiation pattern even in mildly reverberant rooms. A simple tracking system, composed of a depth map camera and a gyroscope, is used to track the position and the orientation of the musician with respect to the microphones. Each pose assumed by the violinist contributes to the portion of radiation pattern corresponding to the part of the instrument “exposed” to the plenacoustic camera. A reference microphone mounted in proximity of the violin is used to normalize the energy.

2. NOTATION AND PROBLEM FORMULATION

2.1. Violin coordinate system

As we are interested in estimating the far field radiation, we consider the violin as a point source located in the center of mass of the instrument. This position approximately corresponds to the bridge location, and it is considered as the origin of the violin coordinate system. The coordinate axes are

THIS RESEARCH ACTIVITY HAS BEEN PARTIALLY FUNDED BY THE CULTURAL DISTRICT OF THE PROVINCE OF CREMONA, ITALY, A FONDAZIONE CARIPLO PROJECT, AND BY THE ARVEDI-BUSCHINI FOUNDATION.

oriented as in Fig. 1, with the bridge lying on the $\bar{x}\bar{z}$ plane. In the paper, we will work also with spherical coordinates, i.e. a point \bar{x} is defined by azimuth $\bar{\phi}$, elevation $\bar{\theta}$, and distance \bar{r} from the origin of the reference frame.

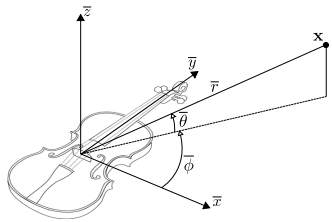


Fig. 1: Violin coordinate system.

2.2. Radiation pattern

The radiation pattern is defined starting from the far field solution of the Rayleigh's first integral [10]. Under the far field assumption, the temporal Fourier transform of the radiated sound field at \bar{x} is given by

$$P(\bar{x}, \omega) = g(\bar{r}, \omega)S(\omega)D(\bar{\phi}, \bar{\theta}, \omega), \quad (1)$$

where $S(\omega)$ is the temporal Fourier transform of the violin source signal, and ω the angular frequency; the Green's function

$$g(\bar{r}, \omega) = \frac{e^{j\frac{\omega}{c}\bar{r}}}{\bar{r}} \quad (2)$$

accounts for the propagation delay and attenuation and c is the speed of sound. The term $D(\bar{\phi}, \bar{\theta}, \omega)$ is the directivity function. The radiation pattern is $|D(\bar{\phi}, \bar{\theta}, \omega)|$, and describes the intensity of the sound field emitted towards direction $(\bar{\phi}, \bar{\theta})$ at frequency ω . For an omnidirectional point source $|D(\bar{\phi}, \bar{\theta}, \omega)| = 1/(4\pi)$.

2.3. Plenacoustic analysis

The goal of this work is to estimate $|D(\bar{\phi}, \bar{\theta}, \omega)|$ at all the frequencies of interest, over a regular grid of angles covering the full spherical domain. To do so, we rely on the plenacoustic analysis [9], a powerful tool for determining the directional components of the sound field at multiple points in space. In particular, this analysis estimates the plane-wave components $L(\mathbf{x}, \mathbf{u}, \omega) \in \mathbb{C}$ propagating towards direction \mathbf{u} and contributing to the sound-field in \mathbf{x} . This goal is achieved by means of space-time processing of data acquired from the plenacoustic camera. Notice that during the performance the violin moves. It is therefore needed to adopt a global reference frame, which is integral with the camera, and for convenience is centered on the bottom-left corner of the camera and oriented as in Fig. 2. We estimate $L(\mathbf{x}, \mathbf{u}, \omega) \in \mathbb{C}$ on a regular rectangular grid defined by points \mathbf{x}_i , $i = 1, \dots, N$, expressed

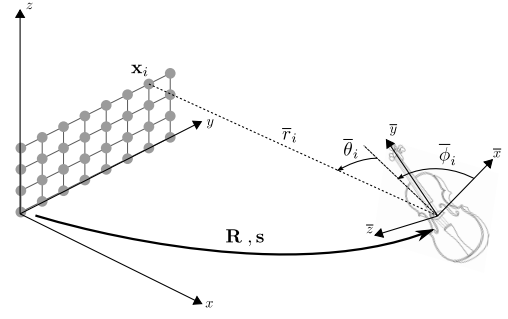


Fig. 2: Plenacoustic analysis.

in the global reference system¹. Let \mathbf{s} be the position of the violin in the global coordinate system, and \mathbf{R} be the 3×3 matrix defining its rotation with respect to the global reference frame. The point $\mathbf{x}_i = [x_i, y_i, z_i]^T$ in the violin coordinate system is

$$\bar{\mathbf{x}}_i = [\bar{x}_i, \bar{y}_i, \bar{z}_i]^T = \mathbf{R}^{-1}(\mathbf{x}_i - \mathbf{s}). \quad (3)$$

The spherical coordinates of $\bar{\mathbf{x}}_i$ are $\bar{\phi}_i, \bar{\theta}_i, \bar{r}_i$ and can be easily computed from $\bar{\mathbf{x}}_i$. Under the assumption that only the violin is present on the acoustic scene, we have that the plenacoustic function at \mathbf{x}_i is given by

$$L(\mathbf{x}_i, \mathbf{u}_i, \omega) = P(\bar{\mathbf{x}}_i, \omega) = g(\bar{r}_i, \omega)S(\omega)D(\bar{\phi}_i, \bar{\theta}_i, \omega), \quad (4)$$

where \mathbf{u}_i is the direction of the ray originating at \mathbf{s} and passing through \mathbf{x}_i . The radiation pattern is obtained from (4) as

$$\begin{aligned} |D(\bar{\phi}_i, \bar{\theta}_i, \omega)| &= \left| \frac{L(\mathbf{x}_i, \mathbf{u}_i, \omega)}{g(\bar{r}_i, \omega)S(\omega)} \right| \\ &= \|\mathbf{x}_i - \mathbf{s}\| \frac{|L(\mathbf{x}_i, \mathbf{u}_i, \omega)|}{|S(\omega)|}. \end{aligned} \quad (5)$$

3. DIRECTIVITY ESTIMATION

In this Section we describe the proposed method for obtaining $|D(\bar{\phi}_i, \bar{\theta}_i, \omega)|$ from the integration of data retrieved from the plenacoustic camera; the reference microphone; and the tracking system. All the measurement devices are mutually synchronized, in order to obtain consistent data.

3.1. Reference microphone

A reference signal $s(t)$ is captured by a microphone located close to the bridge of the violin. As the violin moves and the sound changes during the musical performance, we operate a short-time analysis on $s(t)$. We assume the violin as static and $s(t)$ as stationary during the K samples long observation window. The extracted frame is $s_v(n)$, where n is the

¹Primitives in the violin and global reference frames are identified by \cdot and $\bar{\cdot}$ symbols, respectively

discrete-time index and v is the frame index. In order to discard frames not associated to a violin sound, or with a poor signal-to-noise-ratio, we perform a frame selection. At this purpose, for each frame we compute the short-time energy

$$e_v = \sqrt{\frac{1}{K} \sum_{n=0}^{K-1} s_v(n)^2} \quad (6)$$

and the harmonic ratio HR_v , computed using Eq.(2.33) in [11]. The value $\text{HR}_v = 1$ is reached for purely harmonic frames. The v th frame is selected if and only if $e_v \geq T_e$ and $\text{HR}_v \geq T_{\text{HR}}$, where T_e and T_{HR} are prescribed acceptance thresholds. For acceptable frames, we compute the energy of the signal at the frequency bins ω_k , to obtain $S_v(\omega_k)$.

3.2. Tracking system

In this paragraph we describe the two components of the tracking system, namely an Inertial Measurement Unit (IMU) and a depth map camera. Both the devices are synchronized with the audio recording device. Therefore, all the measurements can be related to the current audio frame v .

3.2.1. IMU

A 9-degrees-of-freedom IMU device is used to determine the orientation of the instrument. The device is attached to the chin-rest and positioned such that its local reference frame is oriented as in Fig. 1. The orientation of the violin at frame v is retrieved through the Euler angles, i.e. yaw α_v , pitch β_v , and roll γ_v , as in [12]. From the Euler angles it is possible to retrieve the rotation matrix \mathbf{R}_v at frame v .

3.2.2. Depth map camera

In order to track the violin position with respect to the global coordinate system, we employ a Microsoft Kinect. The Kinect produces a depth map that is used to fit the skeleton model of the violin player. We estimate the back edge of the chin rest as the middle point between the head and neck joints of the skeleton model. The bridge location is then estimated as the middle point along a segment starting from the chin-rest, of length 34 cm and oriented as the \bar{y} axis of the violin.

3.3. Plenacoustic camera

The ideal plenacoustic camera is implemented by $N_r \times N_c = N_m$ omnidirectional microphones placed on a regular grid, all synchronized with the reference one located on the violin. We group the microphones in subarrays of $M = 3 \times 3$ sensors each. Sub-arrays are maximally overlapped, i.e. $N = (N_r - 2) \times (N_c - 2)$ sub-arrays are available. Let \mathbf{x}_i be the center of the i th subarray, and \mathbf{m}_{ij} , $j = 1, \dots, M$, the positions of the sensors within the subarray. The plenacoustic function is

estimated through delay-and-sum beamforming [13]. More specifically, we estimate the energy radiated along direction

$$\mathbf{u}_i = \frac{\mathbf{x}_i - \mathbf{s}_v}{\|\mathbf{x}_i - \mathbf{s}_v\|} \quad (7)$$

through the pseudo-spectrum $\psi_v(\mathbf{x}_i, \mathbf{u}_i, \omega)$, computed as in [14]. The magnitude of the plenacoustic function is given by

$$|L_v(\mathbf{x}_i, \mathbf{u}_i, \omega)| = \sqrt{\psi_v(\mathbf{x}_i, \mathbf{u}_i, \omega)}. \quad (8)$$

3.4. Data integration

Once we have processed the frame v , we obtain a set of samples of the radiance pattern $|D(\bar{\phi}, \bar{\theta}, \omega)|$. More specifically, we obtain the following samples:

$$|D_v(\bar{\phi}_i, \bar{\theta}_i, \omega_k)| = \|\mathbf{x}_i - \mathbf{s}_v\| \frac{|L_v(\mathbf{x}_i, \mathbf{u}_i, \omega_k)|}{|S_v(\omega_k)|}, \quad (9)$$

for $i = 1, \dots, N$. In order to be robust against measurement noise, we consider only the frequency bins ω_k corresponding to the harmonic peaks in the spectrum whose energy is not below 20 dB that of the main peak. We conclude the measuring session when the violinist moved and rotated in such a way that the radiance pattern has been estimated on the whole 3D angular domain. The gathered data is finally averaged and interpolated to obtain the full 3D pattern, sampled on a regular grid of $N_\phi \times N_\theta = 72 \times 36$ angular positions.

4. RESULTS

In order to assess the accuracy of the estimation, we measured the radiation pattern of two different types of acoustic sources. First the pattern of a commercial loudspeaker has been measured in order to validate the methodology. Then we estimated the radiation pattern of a standard full-size student violin.

4.1. Acquisition setup

Experiments were conducted in a low-reverberation chamber, with reverberation time $T_{60} \approx 50$ ms. We used a T-Bone Ovid CC 100 super-cardioid condenser transducer to measure $|S(\omega)|$. The plenacoustic camera has been realized using 32 Beyerdynamics MM1 measurement microphones, characterized by a flat frequency response and by a omnidirectional polar pattern. The microphones are arranged on a 4×8 grid, thus $N = 2 \times 6 = 12$ sub-arrays are available. The microphone spacing is 7 cm in both the horizontal and vertical directions, corresponding to a spatial aliasing frequency of about 2.5 kHz. The Kinect was placed in a calibrated position below the plenacoustic camera. The recording sampling frequency was set to 48 kHz. Audio frames were extracted using a Hann window of $K = 8192$ samples, with 50% overlap. The acceptance thresholds defined in Sec. 3.1 were set to $T_{\text{HR}} = 0.8$ and $T_e = 0.25$.

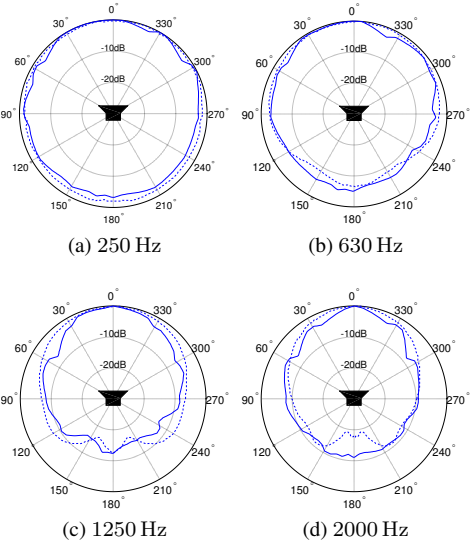


Fig. 3: Genelec 1029A: measured pattern (continuous line) vs reference pattern (dashed line).

4.2. Radiation of a commercial loudspeaker

We measured the horizontal radiation pattern of a Genelec 1029A speaker. Its location is known and it is at a distance of 1.5 m from the plenacoustic camera. The speaker is positioned on a Outline ET250-3D electronic turntable. The acoustic center of the loudspeaker (i.e., the midpoint between the woofer and the tweeter) was at the same height of the camera center. The speaker moved on 36 orientations on the full circle. For each location, it emitted 2 s of white noise. Since orientation of the speaker and energy of the emitted signal are known, we bypassed the frame selection and tracking stages. Comparing the measured pattern with the ground-truth provided by the manufacturer, the resulting average error is below 3 dB in the frequency range 100 Hz - 2.5 kHz. Examples are reported in Fig. 3 at four frequency values.

4.3. Radiation of the violin

We estimated the radiation pattern of a full-size student violin in two different scenarios. First, we instructed the musician to play holding the instrument in predefined positions. Since pose and rotation of the violin were known, we neglected the data coming from the tracking system. Due to the intrinsic limitations in accurately positioning the instrument held by a person, we limited this analysis to the plane $\bar{x}\bar{y}$. The musician stood about 1 m away from the camera, holding the violin with the plate parallel to the floor. We asked him to rotate in 18 angular prescribed positions, pivoting on the bridge. In each position, the violinist played the open D string for approximately 2 s. This way, we obtained a reference measure of the radiation pattern on the horizontal plane. In the second

scenario we tested the whole system. We left the musician free to move, assuming the positions needed for covering the positions of interest, holding the instrument in a standard and fixed location with respect to his head. We asked him to keep each position for about 2 s, while playing the open D string. To avoid unnatural poses, we restricted the analysis to the top half sphere of the radiation pattern ($\bar{z} \geq 0$), corresponding to the front side of the violin.

Results are reported in Fig. 4, where the first row refers to the horizontal plane and the last one shows the full 3D pattern as a function of azimuth $\bar{\phi}$ and elevation $\bar{\theta}$. We show the radiation diagrams of the 5 highest harmonic components of the D note, from 294 Hz (the fundamental frequency) to 2058 Hz (seventh harm.). Diagrams are normalized at each frequency with respect to the maximum energy radiated in all the sensed directions. The dashed line in the first row of Fig. 4 is the pattern obtained in the controlled scenario described before. The very good matching between the measured pattern and the reference one reveals the accuracy of the tracking system.

We observe that, at 294 Hz and 588 Hz, the radiation pattern is mostly omnidirectional, except for a slight energy damping in correspondence of the violinist's head and neck. As the frequency increases, the pattern becomes more directive and exhibits more irregular shapes. This behavior agrees with the predictions and results provided by Weinreich in [2], where the transition from an isotropic to an anisotropic radiation is found to occur approximately at 800 Hz. Indeed, at 1176 Hz there is a clear preferred direction of emission, while at 2058 Hz the pattern presents three main radiation lobes.

Results similar to Fig. 4 are shown in Figs. 4.17-19 of [15]. For instance, the energy damping at 588 Hz in the range $30^\circ - 60^\circ$, in the horizontal plane, is similar to that in Fig. 4.18 of [15] at 550, Hz. Moreover the main direction of emission at 1176 Hz is around 300° in the horizontal plane, which corresponds to that reported in [15]. A similar behavior is also described in [6]. A direct comparison is not possible, as the results in [15] and [6] are relative to different violins. Finally, it is worth noticing that the effect of the body of the musician is visible at all frequencies. However, its impact on the radiation becomes relevant from 882 Hz. This frequency corresponds to a wavelength of 39 cm, which starts to be comparable with the head size.

5. CONCLUSIONS

We have presented a novel methodology to measure the radiation pattern of a violin during the performance, by means of plenacoustic analysis of the radiated soundfield. The radiation pattern is estimated incrementally as the violinist moves and rotates. The directional energy of the soundfield is measured by means of a plenacoustic camera, while the violin position and rotation is tracked through a Kinect and a IMU device. The proposed method presents the advantage of allowing the

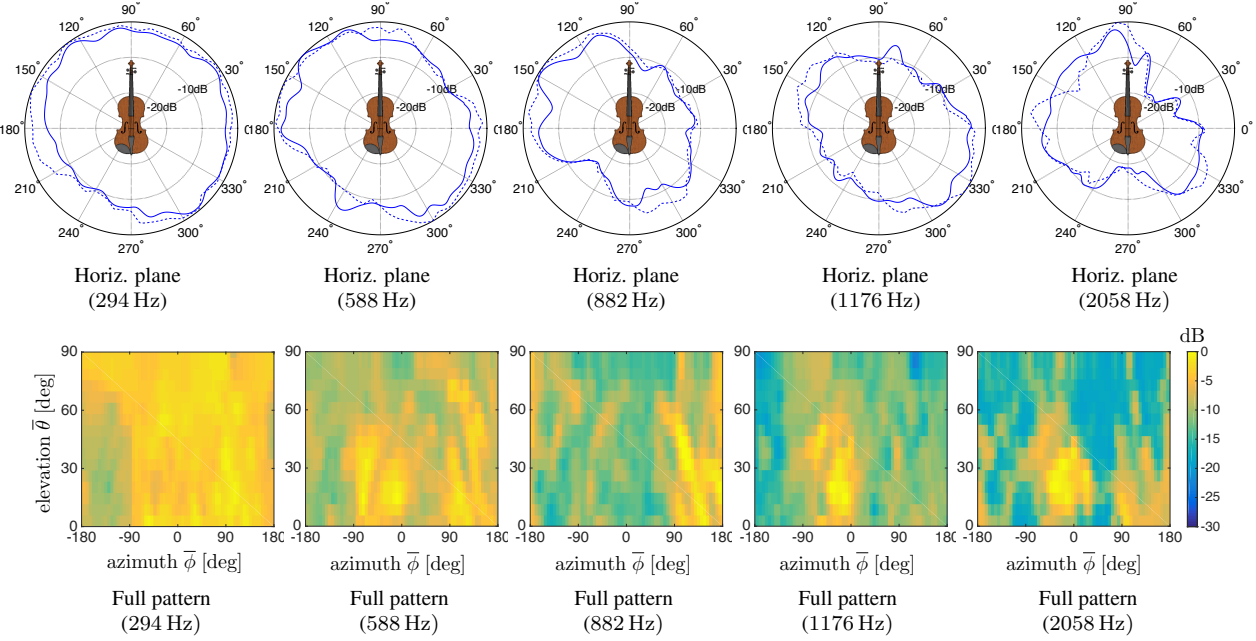


Fig. 4: 3D radiation pattern of the violin under analysis. Results in the horizontal plane are compared with the reference data (dashed line) obtained in a controlled scenario.

musician to play in a more natural fashion, without forcing unnatural poses or playing in anechoic rooms. Moreover, the measurement also includes the effect of the head and body of the player, thus becoming more realistic.

REFERENCES

- [1] G. Bissinger. Some mechanical and acoustical consequences of the violin soundpost. *The Journal of the Acoustical Society of America*, 1995.
- [2] G. Weinrich. Directional tone color. *The Journal of the Acoustical Society of America*, 1997.
- [3] G. Bissinger and J. Keiffer. Radiation damping, efficiency, and directivity for violin normal modes below 4 khz. *The Journal of the Acoustical Society of America*, 2002.
- [4] L. M. Wang and C. B. Burroughs. Acoustic radiation from bowed violins. *The Journal of the Acoustical Society of America*, 2001.
- [5] E. Ravina, P. Silvestri, P. Montanari, and G. De Vecchi. Spherical mapping of violins. *The Journal of the Acoustical Society of America*, 2008.
- [6] J. Pätynen and T. Lokki. Directivities of symphony orchestra instruments. *Acta Acustica united with Acustica*, 2010.
- [7] D. F. Comesana, T. Takeuchi, S. M. Cervera, and K. R. Holland. Measuring musical instruments directivity patterns with scanning techniques. In *International Congress on Sound and Vibration, ICSV*, 2012.
- [8] A. Perez Carrillo, J. Bonada, J. Patynen, and V. Valimaki. Method for measuring violin sound radiation based on bowed glissandi and its application to sound synthesis. *The Journal of the Acoustical Society of America*, 2011.
- [9] D. Markovic, F. Antonacci, A. Sarti, and S. Tubaro. Soundfield imaging in the ray space. *IEEE Transactions on Audio, Speech, and Language Processing*, 2013.
- [10] E. G. Williams. *Fourier Acoustics - Sound radiation and nearfield acoustical holography*. Academic Press, 1999.
- [11] H. G. Kim, N. Moreau, and T. Sikora. *MPEG-7 audio and beyond: audio content indexing and retrieval*. Wiley, 2005.
- [12] S. O. H. Madgwick, A. J. L. Harrison, and R. Vaidyanathan. Estimation of imu and marg orientation using a gradient descent algorithm. In *IEEE International Conference on Rehabilitation Robotics, ICORR*, 2011.
- [13] P. Stoica and R. L. Moses. *Introduction to Spectral Analysis*. Prentice Hall, 1997.
- [14] R. Moses P. Stoica. *Introduction to Spectral Analysis*. Upper Saddle River, NJ: Prentice Hall, 1997.
- [15] J. Meyer. *Acoustics and the performance of music: manual for acousticians, audio engineers, musicians, architects and musical instruments makers*. Springer, PPV Medien, 2009.